Maximum Entropy Spectral Diagnosis Of MHD Generator

Author(s): V. Aoki, T. Seidou, N. Kayukawa, H. Yamazaki, Y. Ozawa, and H. Kitagawa

Session Name: Generators, Part B

SEAM: 23 (1985)

SEAM EDX URL: https://edx.netl.doe.gov/dataset/seam-23

EDX Paper ID: 1114

Maximum Entropy Spectral Diagnosis of MHD Generator

Yoshiaki AOKI, Tadashi SEIDOU, Naoyuki KAYUKAWA,
Hiroki KITAGAWA, Hatsuo YAMAZAKI and Yasutomo OZAWA
Faculty of Engineering, Hokkaido University, Sapporo 060

The maximum entropy method (MEM) was applied to time series intensity data of total light radiation from combustion MHD plasma and the power spectral densities with many characteristic peaks were obtained in the range of a few kHz to ca. 30 kHz, where three criteria, minimizations of The Final Prediction-Error Criterion (FPE), The Akaike's Information Theoretical Criterion (AIC), and The Autoregressive Transfer Function Criterion (CAT), were adopted to determine the optimum prediction-error filter order required for the MEM spectral analysis. Using the MHD flow velocity of 250 m/s obtained from the crosscorrelation function analysis, the frequency spectrum of temperature was transformed to the wave-number dependent power spectral density, in which the $k^{-5/3}$-dependence was found out in the k-range corresponding to the intertial subrange.

§1. Introduction

Spatial and temporal nonuniformities of combustion magnetohydrodynamics (MHD) plasmas significantly cause the degradation of MHD generator performance. Many theoretical and experimental investigations of these nonuniformities have been carried out so far.[1-3] With respect to the spatial nonuniformities, successful studies on flow properties were performed recently[4-9] and interesting results for inherently three-dimensional phenomena were obtained.[4] On the other hand, an experimental investigation of the temporal nonuniformities was carried out by Scott[3] and an analysis of time and frequency spectra was performed based on a stochastic model. However, studies of the temporal fluctuations are scarce and only a beginning has been made in the direction.

A main problem of the analysis of temporal fluctuations is an appropriate choice of algorithm to estimate the spectrum from finite time series data. For this reason, a wide variety of procedures of spectral analysis have been proposed for long.[10-12] With respect to the modern spectral analysis method, the major computational breakthrough occurred with the proposition of the fast Fourier transform (FFT) algorithm by

Cooley-Tukey in 1965.[13] With the development of FFT the field of empirical spectral analysis grew from obscurity to importance and the method now becomes a powerful means for the spectral analysis. However, the fourier transform is insufficient to estimate the precise power spectra from the short time series data. Another important contribution was the introduction of maximum entropy method (MEM) by Burg in 1967.[14] This has a greater, quite often much greater, resolution than other conventional methods and gives more realistic power estimates, especially for shortdata records. In addition, it has turned out that MEM has the same philosophy as autoregression (AR) proposed by Akaike in 1969.[15] However, the application of MEM is reported in a surprisingly small number of papers.

In the preceding paper,[16] the authors obtained several kinds of time series data from the combustion MHD plasma by a light=polarization line-reversal method. these time series data are relatively short data records. then, in the present study, the application of MEM to the time series data was attempted to estimate the time correlation functions and frequency spectral densities and to elucidate the time-dependent characteristics of the plasma flow.

§2. Experimental apparatus and procedures

The experiment was carried out in the propane-oxygen combustion MHD generator at Hokkaido University. The experimental apparatus and procedures are reported in detail in the preceding paper.[16] In the present study, for determining the MHD flow velocity, intensities of total light radiation from the plasma, ϕ_{pl}^{1} and ϕ_{pl}^{2}, were instantaneously measured through two accessholes H_1 and H_2 (Fig. 1), respectively, and, for obtaining the plasma temperature T_P in the vicinity of the electrode, intensities, $\phi_{pl}^{\perp}$, $\phi_{L}^{/\!/}$, and $\phi_{pl+L}^{/\!/}$ were measured through the access hole H_0 (Fig. 1) by the light-polarization line-reversal method,[16] where $\phi_{pl}^{\perp}$ the detected intensity of perpendicular polarization of the plasma emission, $\phi_{L}^{/\!/}$ the detected intensity of linear polarization of the source without the combustion gas and $\phi_{pl+L}^{/\!/}$ the detected intensity of parallel polarization of the plasma emission superimposed on the linear polarization of the source. The access holes H_1 and H_2 were installed at the electrode side wall of the MHD channel, their directions being perpendicular to the direction of the access hole H_0 (Fig. 1). The current flow through the electrode boundary layer J was measured between the electrode pair near H_0 to which electric voltage is externally applied. The electrode is a segmented one which is composed of 20 tantalum lead wires of 0.5 mm diameter and 7 alumina tubes sheath of 3 mm diameter as shown in the inset of Fig. 1. The temperature on the electrode surface was measured to be ca. 1000 K by thermocouples. Measured signals, ϕ_{pl}^{1}, ϕ_{pl}^{2}, $\phi_{pl}^{\perp}$, $\phi_{L}^{/\!/}$, $\phi_{pl+L}^{/\!/}$, and J were stored in 8 kbits wave-memories. The sampling period was 10 μs and the length of each time series data was 1024. In order to investigate a physical picture of

fluctuations in the combustion MHD plasma flow, MEM was applied to time series data of ϕ^1_{pl}, ϕ^2_{pl}, T_P and J.

Plasma temperature T_P was calculated from the following equation,[16]

$$T_p = T_L/\{1 - \frac{\lambda T_L}{C_2} \ln(\frac{K_1 \phi^{\perp}_{pl}}{\phi^{\perp}_{pl} + \phi^{''}_{L} - \phi^{''}_{pl+L}})\}, \qquad (1)$$

where T_L is the temperature of light emitted from the source, λ the wavelength of light, C2 the second radiation constant, K1 the transparency coefficient of incident path between the source and the plasma.

At the first stage, we carried out the experiment under the condition with the externally-applied current flow and with no magnetic field As stated in the preceding paper,[16] the existence of the magnetic field causes current nonuniformities in the transverse directions of the current flow associated with the Hall effect and the secondary flow. These effects much complicate the circumstances and so the experiment with magnetic field will be made at the next stage.

3. Procedure of MEM Spectral Analysis

Mathematical properties of the MEM proposed by Burg[14] have been discussed in detail by Lacoss,[17] Burg,[18] and Ulrych,[19] etc. the algorithm and program for computational procedures of MEM power spectral densities and autocorrelation functions are reported in detail by Andersen,[20] Hino,[21] and Ulrych and Bishop.[22] This section is devoted to a brief summary of MEM spectral estimation of time series data with equal sampling period t.

3.1 Maximum entropy method (MEM)

The MEM power spectrum p(f) (f: frequency), is estimated by[20-23]

$$P(f) = \frac{P_m \Delta t}{\left| 1 + \sum_{k=1}^{m} \gamma_{m,k} \exp(-i2\pi f k \Delta t) \right|^2} \qquad (2)$$

where P_m is the output power of a prediction-error filter of order (or lag) m, and $\gamma_{m,k}$ (m=0,1,2,----,M; k=0,1,2,----,m; m is an optimum filter order) is the corresponding filter coefficients. P_m and $\gamma_{m,k}$ are determined by the equation

$$\begin{pmatrix} R(0) & R(-1) & \cdots\cdots & R(-m) \\ R(1) & R(0) & \cdots\cdots & R(1-m) \\ \vdots & \vdots & & \vdots \\ R(m-1) & R(m-2) & \cdots\cdots & R(-1) \\ R(m) & R(m-1) & \cdots\cdots & R(0) \end{pmatrix} \begin{pmatrix} 1 \\ \gamma_{m,1} \\ \vdots \\ \gamma_{m,m-1} \\ \gamma_{m,m} \end{pmatrix} = \begin{pmatrix} P_m \\ 0 \\ \vdots \\ 0 \\ 0 \end{pmatrix} \qquad (3)$$

This matrix equation is the set of m+1 equations pertaining to a prediction-error filter of order m. R(m) is the autocorrelation function with m, $\gamma_{m,k}$ and P_m.

Eq. (3) can be solved by using Burg's procedure as follow. It begins by first considering the matrix eq. (3) for m=0. The time series data x_n (n=1,2,----,N; n is the data length) is assumed to be the sample function of an ergodic process, so that the time averages are substituted for ensemble averages. We may thus write

$$P_0 = \frac{1}{N} \sum_{n=1}^{N} x_n^2 \qquad (4)$$

$$= R(0),$$

where R(0) is the zero-lag value of the autocorrelation function. In general, after solving eq. (3) up to m-1, the next step m involves a set of m+2 unknowns: $\gamma_{m,k}(k=1,2,----,m)$, R(m), and P_m. thus, in order to solve the matrix eq. (3) of order m+1, an additional criterion is required. Burg proposed that $\gamma_{m,m}$ is determined from minimization of the prediction-error power taken as the average for forward and backward prediction over the entire time interval,[20] that is,

$$\partial P_m / \partial \gamma_{m,m} = 0 , \qquad (5)$$

where

$$P_m = \frac{1}{2(N-m)} \sum_{i=1}^{N-m} [(x_i + \sum_{k=1}^{m} \gamma_{m,k}\, x_{i+k})^2 \qquad (6)$$

$$+(x_{i+m} + \sum_{k=1}^{m} \gamma_{m,k}\, x_{i+m-k})^2].$$

Here, it should be noted that P_m has a minimum value as $\partial^2 P_m/\partial\gamma_{m,m}^2 > 0$. Thus, we obtain

$$\gamma_{m,m} = -2\sum_{i=1}^{N-m} b_{m,i}\, b'_{m,i} / \sum_{i=1}^{N-m} (b_{m,i}^2 + b'^2_{m,i}), \qquad (7)$$

where

$$b_{m,i} = b_{m-1,i} + \gamma_{m-1,m-1}\, b'_{m-1,i},$$

$$b'_{m,i} = b'_{m-1,i+1} + \gamma_{m-1,m-1}\, b_{m-1,i+1},$$

$$b_{0,i} = b'_{0,i} = x_i,$$

and $$b_{1,i} = x_i,\ b'_{1,i} = x_{i+1}.$$

The coefficients $\gamma_{m,k}$ for $k<m$ are determined by the m lower matrix eq. (3) having the well-known solution ($k=0,1,2,\text{----},m-1$), by the use of

$$\gamma_{m,k} = \gamma_{m-1,k} + \gamma_{m,m}\, \gamma_{m-1,m-k}. \qquad (8)$$

In the mth line of eq. (3),R(m) is obtained by

$$R(m) = - \sum_{k=1}^{m} \gamma_{m,k} R(m-k) . \qquad (9)$$

The recursion formula for P_m is derived by inserting eq. (9) in eq. (3),that is,

$$P_m = P_{m-1} (1 - \gamma_{m,m}^2). \qquad (10)$$

Thus, the MEM power spectrum P(f) can be calculated from eq. (2) using the values of P_m and $\gamma_{m,k}$ determined by the above procedure, being carried out from m=0 to an optimum value M. Then, for the autocorrelation function R(m), an extention from of R(m) is used in addition to eq. (9),

$$R(m+l) = - \sum_{k=1}^{m} \gamma_{m,k} R(m-k+l) \qquad (l \geqq 1). \qquad (11)$$

The crosscorrelation function C_{xy} is also estimated from an extended scheme of MEM.[24] In the present study, we use the conventional expression

$$C_{xy}(m\Delta t) = \frac{1}{N-m} \sum_{k=1}^{N-m} x(k)y(k+m), \qquad (12)$$

where x and y are the time series data and m is the number of lag.

3.2 Determination of optimum value M

In MEM, it has been pointed out that,for a given value of record length N, small values of M yield spectral estimates with insufficient resolution,

whereas large values of M yield statistically unstable estimates with spurious details. Thus, the choice of an optimum value of prediction-error filter order is a critical problem, of which circumstance is similar to that well-known in the autoregression (AR). Many workers discussed and proposed several kinds of criteria to choose an optimum value M. Since the choice depends on the statistical properties of the time series under analysis, Haykin and Kesler pointed out that, for the majority of practical measurements where the data can be considered to be short-term stationary, the optimum value M lines in the range from 0.05N to 0.2N.[23] From the similar point of view, Akaike and Nakagawa also reported that $2\sqrt{N} < M < 3\sqrt{N}$.[25] As N=1024, the values of M range from 51 to 205 for the former and those range from 64 to 96 for the latter. these are too rough to determine the value of M.

Here it should be recalled that the spectral density estimate by AR takes on a form being equivalent to MEM estimate.[26,27] Thus, in the present study, we can adopt the following three criteria for the quantitative determination of the magnitude of M often used in AR.

(1) Final Prediction-Error (FPE) criterion:[15] an optimum value M is determined by the minimization of FPE, where FPE is given by

$$FPE(m) = \frac{N+M+1}{N-M-1} P_m. \qquad (13)$$

(2) Akaike's Information theoretical Criterion (AIC):[28] an optimum value M is determined by the minimization of AIC, where AIC is given by

$$AIC(m) = \ln P_m + \frac{2M}{N}. \qquad (14)$$

(3) Autoregressive Transfer Function Criterion (CAT):[29] an optimum value M is determined by the minimization of CAT, where CAT is given by

$$CAT(m) = \frac{1}{N} \sum_{k=1}^{m} \frac{N-k}{NP_k} - \frac{N-m}{NP_m}, \qquad (15)$$

where

$$CAT(0) = -(1 + \frac{1}{N}).$$

With respect to these criteria, some discussions will be made in the section 5.

§4. Reaults

4.1 Time series intensity data

Time-dependent variation of plasma temperature T_P was calculated from eq.(1) using observed time series data $\phi_{pl}^{\perp}$ and $\phi_{pl+L}^{//}$(Fig.2(a)), the magnitude of $\phi_L^{//}$ =160 mV, and other related parameters (T_L=2108 K, λ=7635 Å, C_2=0.01438 mK ,and K_1=0.364), where we used the corrected magnitude of $\phi_L^{//}$ that the obscurity of the windowpane with soot as the burn-up proceeds was compensated with the decreasing of the intensity ϕ_L. The correction procedure for $\phi_L^{//}$ was carried out by applying the condition of the constant optical depth (Fig.2(b)).[16] The corrected time-dependent variation of plasma temperature is shown in Fig.2(c). the averaged value of plasma temperature is 1911 K and its fluctuations are 50 K.

Observed time spectra ϕ_{pl}^1 and ϕ_{pl}^2 are shown in Fig.3(a) and (b), respectively. As clearly seen in the figures, ϕ_{pl}^1 and ϕ_{pl}^2 have very slow oscillations accompanied with a rapidly fluctuations and each averaged level maintains constant during the whole running time: 161.5 mV for ϕ_{pl}^1 and 241.3 mV for ϕ_{pl}^2 . These two sets of data are used to estimate the correlation functions and the power spectral densities.

4.2 Time correlation functions

As described in the preceding section, autocorrelation function are calculated from eqs. (4), (9), and (11) with the optimum filter order M. then, in order to determine M, three criteria (minimizations of FPE, AIC,and CAT) were calculated using the time series data ϕ_{pl}^1 (Fig.3(a)) from eqs. (13), (14), (15), respectively. The calculated FPE, AIC, and CAT associated with the variation of m are shown in Figs. 4(a),(b), and (c), respectively. Minima in the curves FPE and CAT are observed. In FPE (Fig.4(a)), the optimum filter order M ranges from 40 to 59. Cat shows a sharp minimum at m=46 (Fig.4(c)). AIC decreases gradually with m and it has no minimum value (Fig.4(b)). As the result, we safely determined that the optimum filter order M is 50. For the other time series data, we also reached to the same result. Autocorrelation functions R(m) thus calculated

with M=50 are shown in Fig.5(a) and (b) for the time series data ϕ^1_{p1} and ϕ^2_{p1}, respectively. The dependence of autocorrelation functions on m as well as that of power spectral densities will be discussed in the section 5.

Putting the time series data ϕ^1_{p1} and ϕ^2_{p1} into x and y in eq.(12), respectively, crosscorrelation function was calculated (Fig.6). From the result, we obtained a lag time $m_{MAX}\Delta t$=0.44 ms at the maximum in the crosscorrelation function curve. The MHD flow velocity V can be determined by using of $m_{MAX}\Delta t$ and the distance between the access holes H_1 and H_2,

$$V = \frac{L}{m_{MAX}\Delta t} . \qquad (17)$$

is 110 mm in the present study, thus, from eq.(17), the MHD flow velocity was determined to be 250 m/s.

The MHD flow velocity V can be measured by the MHD flowmeter[30] using the relation

$$Vo = VBW \qquad (18)$$

where Vo is the open voltage between the electrode pair, B externally-applied magnetic field, W the width between the electrode pair. In the present study, the magnitude of Vo was measured to be 25.7 V under the condition with B=2.2 teslas and W=0.05 m, and the value of 230 m/s was obtained for V. This supports the value determined from the maximum of crosscorrelation function, thus, we use 250 m/s for the MHD flow velocity in the following analysis.

4.3 Power spectral densities

The power spectral densities of ϕ^1_{p1} for the upper stream (at the position of H_1) and ϕ^2_{p1} for the down stream (at the position of H_2) calculated from eq.(2) using M=50 are shown in Figs. 7(a) and (b), respectively. Characteristic peaks are observed in the frequency range of a few kHz to ca. 30 kHz. The positions of peaks are listed in Table 1. power spectral densities for the interelectrode current and for the plasma temperature are shown in Figs. 8 and 9, respectively. The positions of peaks are also listed in Table 1. From this Table and Fig.7-9, all the spectra have very similar trend with each other on the whole and the following features can be observed. Comparing the upper stream spectrum with the down stream one, the almost peak intensities of the down stream are attenuated except for several peaks at ca. 3 kHz, 5kHz, 9-10 kHz, 18.5-19.5 kHz and 25 kHz. This indicates that the correlation modes observed in

observed in the upper stream side dies away due to gradually increasing disturbances as the flow travels through the MHD channel. Many peaks in the range of 10 30 kHz reappear in the J spectrum though the spectrum belongs to the down stream. This is considered to be due to the effect of Joule heating. In the T_p spectrum peaks also reappear and its cause is of interest.

In order to understand an essential feature of the power spectral density of temperature shown in Fig. 9, we considered the spectral density in a wave number space where the wave number k is defined as k=2 /V. The value of V (=250 m/s) was given in the preceding item. By this transformation, the k-dependent power spectral density of temperature can be represented in Fig. 10. It is noticeable that the $k^{-5/3}$-dependence of the power spectral density is observed in the k-range of a few tens to hundreds m^{-1} corresponding to the so-called inertial subrange. This is supposed to indicate that the combustion MHD plasma flow has a turbulent mode well-known as Kolmogoroff's law.[31,32] The existence of this turbulent mode is reasonable because the Reynolds number Re is sufficiently large in the present MHD flow: Re~10^5 for characteristic scales of velocity ~250 m/s and length ~0.05 m and the kinematic viscosity ~2 cm^2/s in the flow. The large-scale turbulence in the small wave number region (k<a few tens m^{-1}) is considered to be associated with the overall process of combustion of which characteristic length is the scale of MHD channel (ca. 0.03 0.05 m) and the small-scale one in the higher wave number region (k>a few tens m^{-1}) to be associated with several kinds of dynamical characteristics of the MHD plasma flow in smaller time and space.

5. Discussion

5.1 On the determination of the optimum filter order M

Although the superiority of MEM over other conventional spectral estimate methods, in particular for short data lengths,has been recognized so far, the usefulness of this approach is limited to a considerable extent by the lack of a criterion for choosing the optimum prediction error filter order M. In Fig. 11 and 12, MEM autocorrelation functions and power spectral densities for ϕ_{pl}^{1} are shown with the variation of the prediction error filter order m, respectively. as seen in the figures, for too small m, a highly smoothed spectrum is obtained, and, for an excessively large m, spurious detail is introduced into the spectrum. Accordingly, the correct choice of M is required for obtaining a meaningful estimate of the power spectrum as well as of autocorrelation function.

The estimating procedure proposed by Akaike,[15] which is called the final prediction error (FPE, eq. (13)), was the first successful method and its application to MEM spectral analysis can remove the main shortcoming of this technique in some cases. However, the disappearance of the minimum

small minimum was observed though it clearly appeared (Fig.4(a)). The second criterion also proposed by Akaike,[28] called the information theoretical criterion (AIC, eq.(14)), is an important technique which is known as a versatile statistical identification criterion. AIC and FPE are expected to give identical results for M. Unfortunately, the application of AIC to the present data was unsatisfied (Fig.4(b)). thus, a third criterion is required for more distinct determination of M. The third criterion has proposed by Parzen[29] and is known as the autoregressive transfer function criterion (CAT, eq.(15)). this scheme is considered to have similar behavior to AIC. the result of CAT indicated an extremely sharp minimum at the same position of m as that of FPE (Fig. 4(c)). Thus, we can determine that the optimum value M is 50 and it can be safely said that with M=50 the true spectral density (Fig.7) as well as the corresponding autocorrelation function (Fig.5) was obtained by a combination of FPE, AIC, and CAT, though comparative properties of these three criteria required much further study.

5.2 Kolmogoroff's $k^{-5/3}$-law observed in the MHD plasma flow

In the present study, the $k^{-5/3}$-dependence of the power spectrum density is observed in the inertial subrange : a few tens to hundreds m^{-1} (4.3 , Fig.11) . This is well-known as Kolmogoroff's law.[35,36] Very few knowledges have been obtained so far with respect to the turbulence of plasma flow within MHD generator and the law has never ever been found out before. The cause is mainly attributed to the lack of appropriate method for overcoming the experimental difficulties.

Our ascertaining the kolmogoloff's law in the MHD flow has the following significance. From the theoretical point of view, the kolmogoloff's law of $k^{-5/3}$ dependence can be said to be an ideal mode of turbulence.[35,36] That is ,it can be understood that the fundamental model of turbulent flow within the MHD generator is the ideal one like many other ordinary fluids.[35] Thus, we can confirm a reference mode which is extremely useful for detailed elucidation of the turbulence of plasma flow within the MHD generator. This successful result obtained in the present study is essentially brought about by applying the correlation function approach to the analysis of various time series data. Especially, the major reason is attributed to the precise spectrum given by MEM.

5.3 Characteristic frequency peaks in power spectral densities

The MEM power spectral densities accompanied with the characteristic peaks are shown in Fig.7-9. In order to understand the various plasma phenomena in a frequency resolved space, several studies[3,35-38] have been carried out so far with respect to the characteristic peaks, typically associated with arcing, flow turbulence and combustion instabilities. Frequency peaks at 1.5, 5, and 25 kHz were assigned to the arcing by Sadovnik, et al.[37] The arc at 3-6 kHz were also reported by Zalkind, et

al.[35] More recently, turburent modes at 300-600 Hz and combustion instability fluctuations at less than 100 Hz were observed by Vodonos, et al.[38] Thus, characteristic peaks in the frequency range below several tens kHz are of significance.

Comparing the above-mentioned characteristic peaks with the peaks observed in the present study, the following point is noted; the present result shows many peaks in larger frequency range than 2 kHz, including all the peaks considered to be the arc modes. Dynamical properties of MHD flow are supposed to reflect on these peaks, and so the confirmation of these peaks are further required to be made experimentally in addition to the theoretical assignment of those.

5.4 Frequency resolution of MEM power spectral densities

The MEM has been recognized to be a high resolution estimator of power spectral density from several simulation studies[17,22,33] and its frequency resolution is mainly limited by the data length and the sampling time. In the present study, the analyzable power spectral densities are limited at the frequency range reached to 50 kHz with the data length of 1024, and sampling time 10 μs. The frequency resolution Δf in MEM is defined by $\Delta f = 1/l\,\Delta t$, proposed by Blackman-Tukey[34], where l is assumed to be the maximum number of correlation lag or the optimum filter order. Thus, the present frequency resolution f is obtained to be much less than 2 kHz. therefore, it can be said that the peaks shown in Figs.7-9 are well-resolved though some uncertainty remains in the first peaks.

§6.Conclusion

In order to investigate the combustion MHD flow properties, the intensities of total light radiation from the plasma were measured as the time series data in the two separated access holes in the direction of the plasma flow (Fig.2-3). The plasma temperature near the electrode was measured by means of the light-polarization line-reversal method and the averaged temperature was obtain to be 1911 K. The spectral analysis of the data were carried out by the maximum entropy method which is a high resolution estimator of power spectral densities. The value of the optimum filter order was determined to be 50 by a combination of three criteria (minimization of FPE, AIC, and CAT; Fig.4) and with the value of M=50 the autocorrelation function (Fig.5) and the power spectral densities (Fig.7-9) were obtained. The characteristic peaks on which dynamics of the MHD plasma flow reflect were observed in the frequency region of 2-30 kHz. From the crosscorrelation function between the upper time series data and the lower one (Fig.6) the flow velocity of the MHD plasma was obtained to be 250 m/s. Using this value of the flow velocity, the k-dependent power spectral density of temperature (Fig.10) was obtained from its frequency-dependent power spectral density and the $k^{-5/3}$-dependence was observed. In the view-

spectral density of temperature (Fig. 10) was obtained from its frequency-dependent power spectral density and the $k^{-5/3}$-dependence was observed. In the view-point of diagnosis of the MHD plasma, thus, the present study showes a possibility to experimentally investigate the MHD plasma dynamics, though theoretical analysis of time-dependent phenomena in MHD plasma flow are required still more.

References

1) S. A. Self and C. H. Kruger: J.Energy 1 (1977) 25.
2) S. A. Self:AIAA International Meeting & Technical Display "Global Technology 2000 ", Baltimore, 1980 (AIAA, New York, 1980) AIAA-80-0926.
3) M.H. Scott: AIAA 9th Fluid and Plasma Dynamics Conf., San Diego, 1976 (AIAA,New York, 1976) AIAA-76-313.
4) C. D. Maxwell, T. F. Swean, Jr., A. A. Vetter, R. D. Grouse, D. A. Oliver, C. D. Bangerter, and S. T. Demetriades: AIAA14th Fluid and Plasma Dynamics Conf.,Palo Alto, 1981 (AIAA, New York, 1981) AIAA-81-1231
5) S. T. Demetriades, D. A. Oliver, T. F. Swean, and C. D. Maxwell: AIAA 19th Aerospace Sciences Meeting, St. Louis, Missouri, 1981 (AIAA, New York, 1981) AIAA-81- 0248.
6) S. L. Girshick and C. H. Kruger: Proc. 22nd Symposium on Engineering Aspect of Magnetohydrodynamics, Mississippi, 1984, 2.7.1 (MHD Energy Center of Mississippi, 1984).
7) R. K. James and C. H. Kruger: Proc. 18th Symposium on Engineering Aspect of Magnetohydrodynamics, Montana, 1979, E.4.1 (MHD Energy & MHD Reserch & Development Institute, Inc., Montana, 1979).
8) M. Ishikawa and J.Umoto: Proc. 22nd Symposium on Engineering Aspect of Magnetohydrodynamics, Mississippi, 1984, 2.8.1 (mhd Energy Center of Mississipi State University, Mississipi,1984).
9) S. P. Vanka and R. K. Ahlumalia: J. Energy, 7 (1983) 65.
10) D. E. Childer: Modern Spectrum Analysis (IEEE press, New York, 1978).
11) S. Haykin, ed. : Nonlinear Method of Spectral Analysis (Springer-Verlag, Berlin Heidelberg, 1979).
12) D. R. Brillinger and P. R. Krishnaiah, ed.:Time Series in the Frequency Domein (North-Holland, Amsterdam, 1983).
13) J. W. Cooley and J. W. Tukey: Math. Compt., 19 (1965) 297.
14) J. P. Burg: Proc. 37th Meeting of the Society of Exploration Geophysicist, Oklahoma City, Okla (1967); reprinted in ref.10, p.34
15) H.Akaike: Ann. Inst. Statist. Math. 21 (1969) 243 and 407.
16) Y. Aoki, T. Seidou, and N.Ohtomo: Jpn. J. Appl. Phys., 23 (1984) 1487
17) R. T. Lacoss: Geophysics, 36 (1971) 661; reprinted in ref.10 p.134
18) J. P. Burg:NATO Advanced Study Institute on Signal Processing with Emphasis on Underwater Acoustic, Enschede, Netherlands, 1968; reprinted in ref.10, p.42.
19) T. J. Ulrych: J.Geophys., 77 (1972) 1396
20) N. Andersen: Geophys., 39 (1974) 69; reprinted in ref.10, p.252
21) M.Hino: Spekutoru Kaiseki (Spectrum Analysis) (Asakurashoten, Tokyo, 1974) (in Japanese)
22) T. J. Ulrych and T. N. Bishop: Rev. Geophysics and Space Phys. 13 (1975)183; reprinted in ref.10, p.54.

23) S. Haykin and S. Kesler: in ref.11,p.9.
24) A. H. Nuttal: Naval Underwater System Center Tech. Report 5729 (1976).
25) H. Akaike and T. Nakagawa: Dainamikku Shisutemu no Toukeiteki Kaiseki to Seigyo (Statistical Analysis and Control of Dynamic system) (Saiensu sha, Tokyo, 1972) (in Japanese).
26) A. van den Bos: IEEE Trans. Inform. Theory, IT-17 (1971) 493; reprinted in ref.10, p.92.
27) E.Parzen: Multivariate Analysis II (Academic Press, New York, 1967), ed., P. R. Krishnaiah.
28) H. Akaike: IEEE Trans. Autom. Contr. AC-19 (1974) 716.
29) E. Parzen: IEEE Trans. Autom. Contr. AC-19 (1974) 723.
30) M. M. Micci and L. H. Caveny: AIAA J. 20 (1982) 516.
31) A. S. Monin and A. M. Yaglom: Statistical Fluid Mechanics of Turbulence, vol.1 and 2 (The MIT Press, Cambridge, 1975).
32) S. Chandrasekhar: Proc. Roy. Soc., A233 (1955) 322.
33) H. R. Radoski, P. F. Fougere, and E. J. Zawalick: J. Geophys. Res., 80 (1975) 619.
34) R. B. Blackman and J. W. Tukey: The Measurement of Power Spectra from the Point of Communication Engineering (Dover Publications Inc., New York , 1958)
35) V. I. Zalkind, V. V. Kirillov, Yu. A. Larionov, and N. S. Semenov: J. Appl. Mechanics and Technical phys.,11 (1970) 130.
36) V. I. Kovbasyuk, N. N. Baranov, A. D. Iserov, and I. I. Klimovskii: High Temp., 15 (1977) 1110.
37) I. Sadovnik, M. Martinez-Sanchez, and a. Solbes: Proc. 19th Symposium on Engineering Aspect of Magnetohydrodynamics, Tennessee, 1981, 10.1.1 (The University of Tennessee Space Institute,Tenessee, 1981).
38 Ya. I. Vadonos, Yu. V. Makarov, and O. I. Obrezkov: High Temp., 21 (1983) 140.

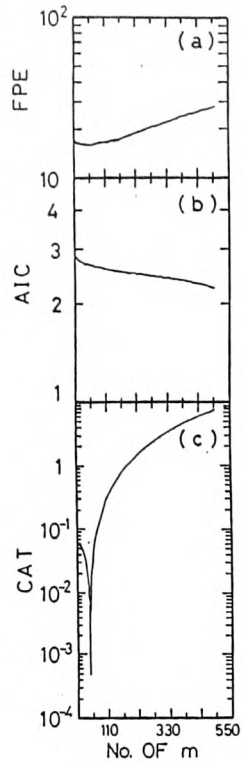

Fig. 4. Three kinds of MEM criteria calculated for the time series data of ϕ^1_{p1} with variation of m, (a) FPE, (b) AIC, (c) CAT.

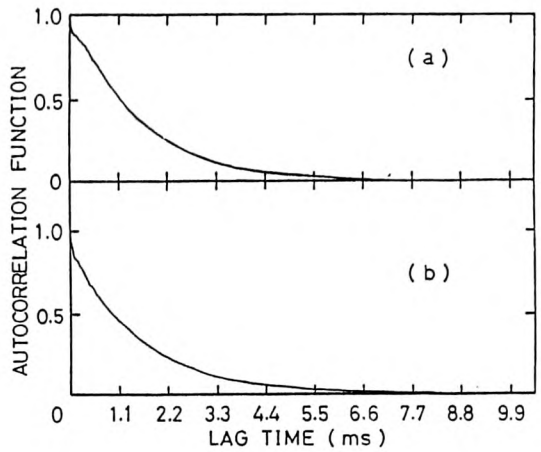

Fig. 5. MEM autocorrelation functions for (a) ϕ^1_{p1}, and (b) ϕ^2_{p1}.

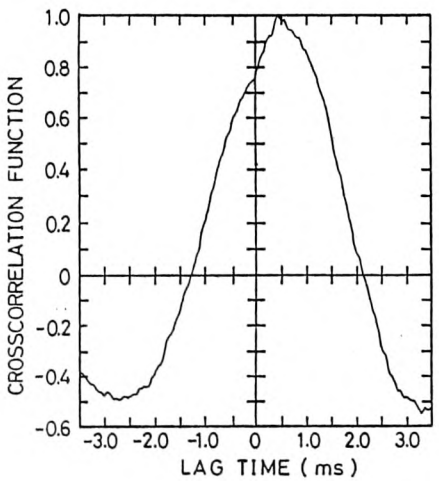

Fig. 6. Crosscorrelation function between the upper stream spectrum and the lower one.

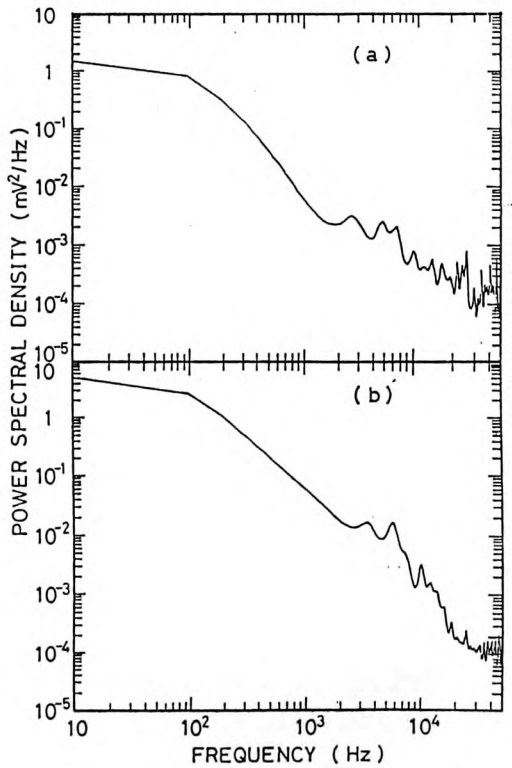

Fig. 7. MEM power spectral densities with an optimum filter order M=50 for (a) ϕ^1_{p1}, and (b) ϕ^2_{p1}.

Table I. The position of peaks (kHZ).

	Upper stream	Down stream		
	ϕ^1_{pl}	ϕ^2_{pl}	J	T_p
1	2.6	3.0	2.9	2.3
2	4.8	5.5	(5.2)	4.6
3	6.4	(6.7)	6.5	6.4
4	8.8	10.1	9.6	8.8
5	(10.9)	----	----	----
6	12.7	(12.0)	11.4	12.3
7	----	(13.5)	14.0	14.7
8	15.5	(15.6)	16.0	16.8
9	(18.4)	18.4	19.6	19.1
10	20.9	20.4	----	----
11	23.3	(22.3)	23.0	21.9
12	25.0	24.4	----	24.6
13	(27.0)	(26.8)	26.6	26.6
14	29.1	(28.8)	29.5	28.9
15	(31.8)	(32.2)	(32.0)	31.3

( ): weak

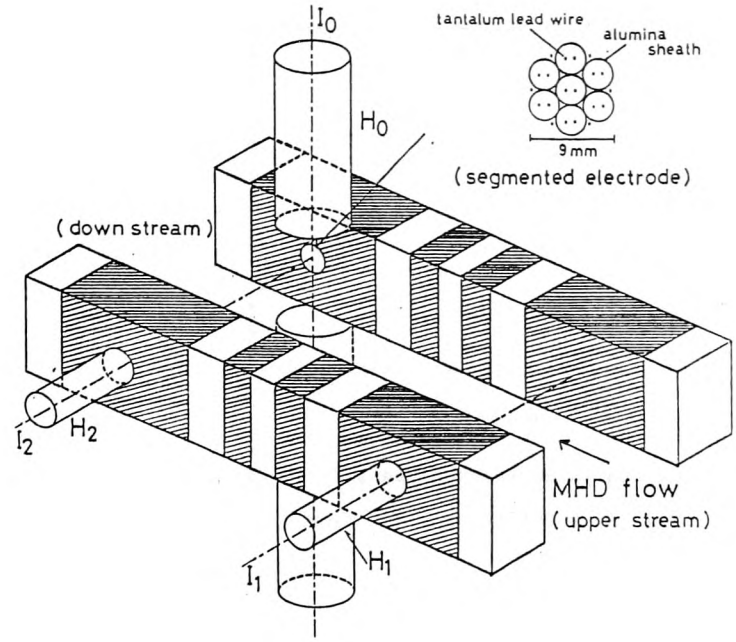

Fig. 1. Perspective view of MHD channel with three access holes. Segmented electrode is shown in the inset. H_0, H_1, H_2: Access holes, I_0, I_1, I_2: Light axises, Hatched: Water-cooled electrode, Unhatched: MgO insulator.

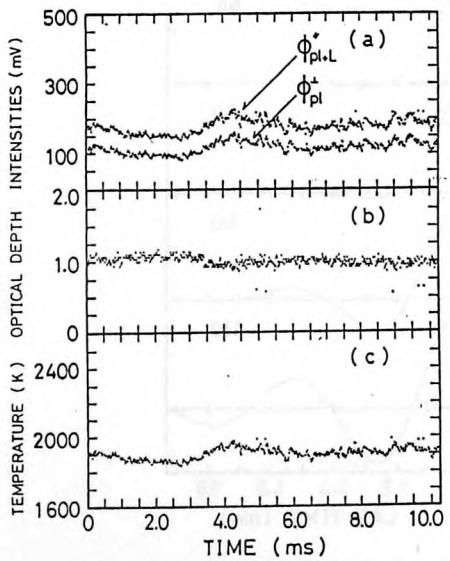

Fig. 2. (a) Measured time-spectra of plasma light intensities ϕ_{pl}, ϕ_{pl+L}, (b) Optical depth τ_λ, (c) Temperature variation T_p.

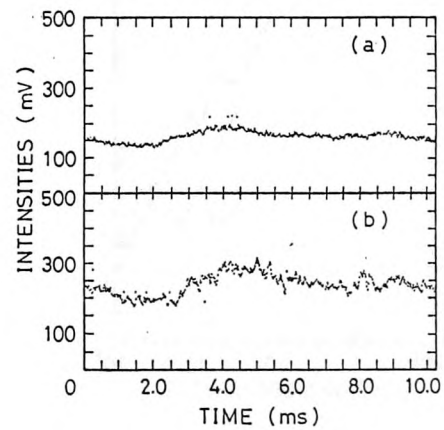

Fig. 3. Time-spectra of intensities of total light radiation from the plasma. (a) the upper stream, (b) the down stream.

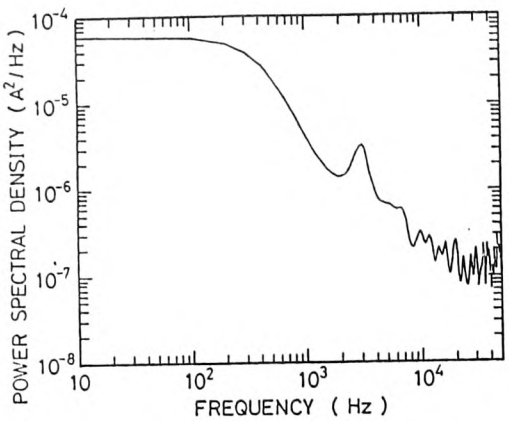

Fig. 8. MEM power spectral density (M=50) for the electric current flow J.

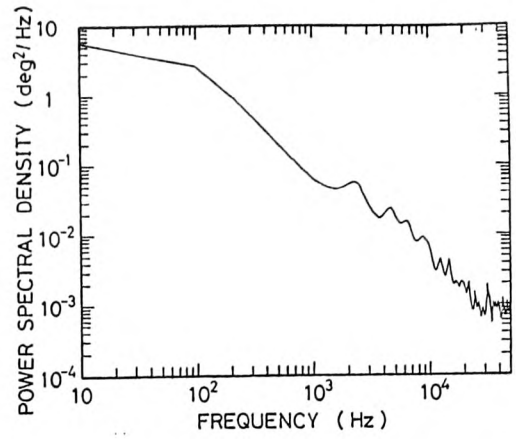

Fig. 9. MEM power spectral density (M=50) for the temperature T_p.

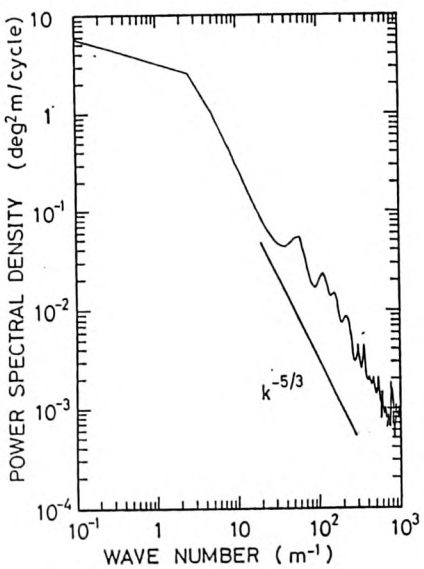

Fig. 10. Wave-number dependent power spectral density of temperature.

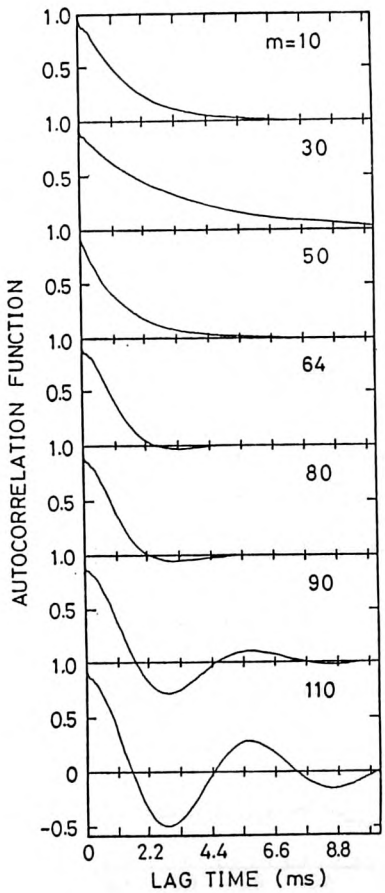

Fig. 11. MEM autocorrelation function for ϕ^1_{p1} with variation of m (10, 30, 50, 64, 80, 96, and 110 from upper figure to down one).

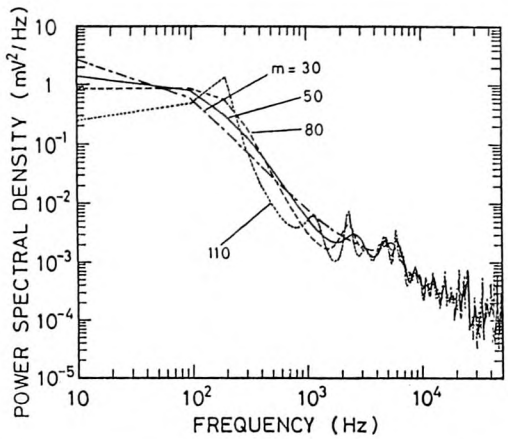

Fig. 12. MEM power spectral densities for ϕ_{p1}^{1} with variation of m

— - — : m=30, ——— : m=50, - - - - -: m=80, ·····: m=110.